Available online at www.sciencedirect.com
SCIENCE DIRECT
Tectonophysics 417 (2006) 141–153
TECTONOPHYSICS
www.elsevier.com/locate/tecto

Physical and stochastic models of earthquake clustering

Rodolfo Console *, Maura Murru, Flaminia Catalli

Istituto Nazionale di Geofisica e Vulcanologia, via di Vigna Murata 605, 00142, Rome, Italy

Received 26 August 2004; accepted 17 May 2005
Available online 3 March 2006

Abstract

The phenomenon of earthquake clustering, i.e., the increase of occurrence probability for seismic events close in space and time to other previous earthquakes, has been modeled both by statistical and physical processes.

From a statistical viewpoint the so-called *epidemic model* (ETAS) introduced by Ogata in 1988 and its variations have become fairly well known in the seismological community. Tests on real seismicity and comparison with a plain time-independent Poissonian model through likelihood-based methods have reliably proved their validity.

On the other hand, in the last decade many papers have been published on the so-called Coulomb stress change principle, based on the theory of elasticity, showing qualitatively that an increase of the Coulomb stress in a given area is usually associated with an increase of seismic activity. More specifically, the *rate-and-state* theory developed by Dieterich in the ′90s has been able to give a physical justification to the phenomenon known as *Omori law*. According to this law, a mainshock is followed by a series of aftershocks whose frequency decreases in time as an inverse power law.

In this study we give an outline of the above-mentioned stochastic and physical models, and build up an approach by which these models can be merged in a single algorithm and statistically tested. The application to the seismicity of Japan from 1970 to 2003 shows that the new model incorporating the physical concept of the rate-and-state theory performs not worse than the purely stochastic model with two free parameters only. The numerical results obtained in these applications are related to physical characters of the model as the stress change produced by an earthquake close to its edges and to the A and σ parameters of the rate-and-state constitutive law.

Keywords: Earthquake interaction; Rate-and-state; Triggering; Clustering; Epidemic model; Likelihood

1. Introduction

Seismicity appears to the observers as a kind of macroscopic behavior of the Earth as a complex system. Universal laws are generally applicable to populations of earthquakes: an example is their magnitude distribution, known as Gutenberg–Richter (G–R) law. A second example is the time decay of the occurrence rate in aftershock sequences, known as Omori law.

Here we are challenged by the problem of understanding the microscopic properties of the Earth that can explain the observed behavior of seismicity. In this respect we start from the analysis of one of the most universal features characterizing seismic activity: earthquake clustering. The concept of clustering includes not only the trend of earthquakes of occurring densely grouped in relatively small spatial and temporal volumes, as in foreshock and aftershock series, but

* Corresponding author.
E-mail addresses: console@ingv.it (R. Console), murru@ingv.it (M. Murru), catalli@ingv.it (F. Catalli).

0040-1951/$ - see front matter © 2005 Elsevier B.V. All rights reserved.
doi:10.1016/j.tecto.2005.05.052

also other less evident long term rate variations, phenomenologically denoted as seismic quiescence, seismic acceleration or earthquake triggering episodes. All these non-random features testify the existence of physical interaction between earthquake sources. Thus, studying the space–time interaction of earthquakes is important for the comprehension of the phenomenon of earthquakes itself. It might have possible applications in the mitigation of earthquake risk too.

A purely statistical approach to this phenomenon exists with the name of *epidemic model*, or ETAS (Ogata, 1988, 1998; Console and Murru, 2001; Console et al., 2003). In the epidemic models each earthquake source is supposed capable of increasing the probability of new earthquakes according to a common space and time probability distribution decreasing from the source. However, despite they provide a reasonably good statistical representation of earthquake interaction, their physical interpretation is ignored.

In order to formulate a more physical description of the clustered seismicity, we consider that seismic events modify the stress field around the causative fault. Some recent studies put in evidence that sudden stress variations, even of small magnitude, can produce large variations of the seismicity rate. It is recognized as a phenomenon of triggering, rather than induction, on faults that are already in critical state. The seismic rate increases in general where the stress change (called Coulomb stress change) is positive, according to the Coulomb model (Mendoza and Hartzell, 1988; Boatwright and Cocco, 1996; Stein and Barka, 1997; Gomberg et al., 1998, 2000; Toda et al., 1998; Harris, 1998; Stein, 1999; Gomberg, 2001; King and Cocco, 2001; Kilb et al., 2002; Belardinelli et al., 2003). These studies were able to give a physical interpretation for earthquake interaction observed in specific real cases, but were not suitable for modeling the usual time decay of the aftershock rate after a mainshock. In fact, in this simple model all the aftershocks should occur instantaneously at the time of the arrival of seismic waves, if the static stress exceeds a threshold stress given by the Coulomb–Amonton criterion. The experience shows that the Earth doesn't rather behave in this way. The most popular empirical description of the aftershock phenomenon, the Omori law, states that the aftershock rate decays in time as t^{-1}. Among the various theories modeling the Omori law, we have taken in consideration only the one that involves a particular constitutive behavior of faults. Therefore, we have not considered, even without rejecting them in principle, other hypotheses that predict a time variation in stress, like viscoelasticity and diffusion of fluids in the medium. The rate-and-state model for earthquake nucleation introduced by Ruina (1983) and Dieterich (1986, 1992, 1994) seems capable of substantially explaining all the phenomenology (e.g., Helmstetter et al., 2005). In this model slip doesn't occur instantaneously at the exceeding of a threshold stress as for the Coulomb–Amonton criterion, but follows a more complex time history with various phases. Following the rate-and-state model it has recently been possible to simulate seismicity quite realistically, accounting for the rate of events induced by stress changes even at large distance from the inducing earthquake (Ziv and Rubin, 2003; Ziv, 2003).

Interesting examples of studies by which stress changes are linked to seismicity rate changes using the rate-and-state model are given by Dieterich et al. (2000) and Toda et al. (2002). In both examples the authors applied the model to stress changes produced by volcanic intrusions, with clearly observable consequences on the seismic activity in the surrounding areas. We are following here a different approach, pursuing a model where very few physical parameters are capable of modeling seismic activity as reported in a usual seismic catalog, without any additional data obtainable only in particular circumstances.

In this paper we first review the principles of stochastic models for earthquake clustering. Then we introduce a new formulation of the Dieterich rate-and-state model that allows its application to modeling earthquake clustering. In this way we obtain a new stochastic model with a limited number of empirical free-parameters. By means of a test based on Japanese seismicity (collected by the Japan Meteorological Agency from 1970 to 2003), we show that the new stochastic model preserves the capability of describing the observations with high likelihood.

2. Stochastic model for earthquake clustering

In a stochastic model, earthquakes are regarded as the realization of a point process. Each event is characterized by its location-time-magnitude coordinates (x, y, t, m). Here, as in other applications (Console and Murru, 2001; Console et al., 2003) we neglect depth from the spatial coordinates of earthquakes.

We assume that the G–R law describes the magnitude distribution of all the earthquakes in a sample, with a constant β-value (β is linked to the b-value of the G–R law by the relation $\beta = b\ln(10)$), independently of the space coordinates. If we neglect the interactions between events, and assuming that the earthquake occurrence is a process with no memory and

time independent rate, the space density of earthquakes of magnitude equal to or larger than m is expressed as

$$\mu(x,y,m) = \mu_0(x,y)\mathrm{e}^{-\beta(m-m_0)}, \quad (1)$$

where $\mu_0(x,y)=\mu(x,y,m_0)$ is the space density of earthquakes of magnitude equal to or larger than m_0. The density magnitude distribution of earthquakes, obtained from Eq. (1), is:

$$\lambda_0(x,y,m) = \mu_0(x,y)\beta\mathrm{e}^{-\beta(m-m_0)}. \quad (2)$$

In both Eqs. (1) and (2) the choice of m_0 is not critical, provided that the set of data is complete above it.

Taking more in general into account the influence of the previous inducing earthquakes, the expected resultant rate density of seismic events can be written as (Ogata, 1998; Console and Murru, 2001, Console et al., 2003):

$$\lambda(x,y,t,m) = f_{\mathrm{r}}\cdot\lambda_0(x,y,m) + \sum_{i=1}^{N} H(t-t_i)\cdot\lambda_i(x,y,t,m), \quad (3)$$

where f_{r} is the *failure rate* (i.e., the fraction of events that occurs spontaneously), $\lambda_0(x,y,m)$ represents the background seismicity expressed as in (2), t_i is the occurrence time of the earthquakes, the total number of which is N, $H(t)$ is the step function, and $\lambda_i(x,y,t,m)$ is the single contribution of the previous earthquakes.

Eq. (3) expresses the popular concept of the ETAS model (Ogata, 1988). The rate density corresponding to any earthquake is, in general, constituted by the superposition of the first and the second terms on the right-hand of (3). In this way, as in a fuzzy system, no earthquake is claimed to be fully linked to any other earthquake in particular, but rather to all previous events, and to the background seismicity, with different weights.

To build up a purely stochastic model, we hypothesize that the contribution of any previous earthquake (x_i, y_i, t_i, m_i) to the occurrence rate density of the subsequent earthquakes is decomposable (for $t>t_i$) into three terms, respectively representing the time, magnitude and space distribution, as:

$$\lambda_i(x,y,t,m) = K\cdot h(t-t_i)\cdot\beta\mathrm{e}^{-\beta(m-m_i)}\cdot f(x-x_i,y-y_i), \quad (4)$$

where K is a constant parameter, while $h(t)$ and $f(x,y)$ are the time and space distributions, respectively.

For the time dependence we adopt the so-called modified Omori law (Ogata, 1983):

$$h(t) = (p-1)c^{(p-1)}(t+c)^{-p} \quad (p>1), \quad (5)$$

where c and p are characteristic parameters of the process, and the expression is normalized so that $\int_0^\infty h(t)\,\mathrm{d}t=1$. In this context Eq. (5) is used not only for first generation aftershocks but also for secondary aftershocks triggered by subsequent earthquakes.

For the spatial distribution of the induced seismicity we consider two different forms. The first is represented by a function, normalized to 1, with circular symmetry around the point of coordinates (x_i, y_i). This function in polar coordinates (r, θ) can be written as

$$f(r,\theta) = \frac{q-1}{\pi}\cdot\frac{d^{2(q-1)}}{(r^2+d^2)^q} \quad (6a)$$

where r is the distance from the point (x_i, y_i) and d and q are two free parameters (Console et al., 2003).

The second form, still represented by an isotropic inverse power of the distance, with circular symmetry around the epicenter of the triggering earthquake, includes the dependence on the magnitude of the previous events by scaling the parameter d with the magnitude:

$$f(r,\theta) = \left(\frac{d_i^2}{r^2+d_i^2}\right)^q. \quad (6b)$$

where $d_i=d_0\mathrm{e}^{\alpha(m_i-m_0)}$. In this case $f(r,\theta)$ is not normalized, and m_i in Eq. (4) must be substituted with m_0.

Eqs. (4), (5), and (6a)–(6b) define the stochastic models named ETASa and ETASb, respectively, in the following of the paper. The free parameters for model ETASa are K, c, p of the generalized Omori formula, and d and q of the space distribution of triggered events. In model ETASb a further free parameter α is added (Zhuang et al., 2004). β (or b) is obtained from the catalog data by the maximum likelihood method, independently of the other adjustable parameters.

3. Application of the rate-and-state model to earthquake clustering

For building up a new clustering model, hereinafter named Epidemic Rate-and-State (ERS) model, we assume that the temporal behavior of the seismicity triggered by a Coulomb stress change in an infinite population of faults is described by the rate-and-state model introduced by Ruina (1983) and Dieterich (1986, 1992, 1994). According to Dieterich (1994) the rate $R(t)$ of earthquakes after a $\Delta\tau$ stress change at time $t=0$ is

given by:

$$R(t) = \frac{R_0}{1-\left[1-\exp\left(\frac{-\Delta\tau}{A\sigma}\right)\right]\exp\left(\frac{-t}{t_a}\right)} \quad (7)$$

where R_0 is the previous background rate density, $\Delta\tau$ is the stress change, and A, σ and t_a are parameters of the constitutive law. Dieterich (1994) has shown that the characteristic time, t_a (the time at which the rate returns back to the background value), is related to the stress rate, $\dot{\tau}$, of the area by the relation:

$$t_a = \frac{A\sigma}{\dot{\tau}}. \quad (8)$$

Note that both $R(t)$ and R_0 express the number of earthquakes with magnitudes exceeding a given threshold, m_0, in a unit space and time volume.

It is easily understandable from Eq. (7) that the integral of $R(t)$ over infinite time diverges. This is related to the fact that the limit of $R(t)$ for $t\to\infty$ is the background rate, R_0. With the aim of introducing the rate-and-state model expressed by Eq. (7) in the epidemic model described in Eqs. (3) and (4), we prefer to deal with the net triggered seismicity rate $R'(t)=R(t)-R_0$. The plot of $R'(t)$ versus time for different values of $\Delta\tau$ is shown in Fig. 1. It shows that the initial value of the triggered seismicity rate immediately after the triggering event is proportional to the exponential of the stress variation $\Delta\tau$ but the time period over which $R(t)$ is maximum and relatively constant decreases exponentially by the same factor for increasing stress change. This time period, in substantial agreement with Dieterich (1994), can be obtained computing the intersection between $R'(t=0)$ and the straight line corresponding to the limit of $R'(t)$ when $\Delta\tau\to\infty$. Such time period ranges from few hours for a variation $\Delta\tau=5$ MPa to several years for $\Delta\tau=1$ MPa.

The integration of $R'(t)$ over time from 0 to ∞ leads to the result that the total number of triggered events in an area of constant stress change is proportional to $\Delta\tau$ (Console and Catalli, submitted for publication; Helmstetter et al., 2005):

$$\int_0^\infty R'(t)\mathrm{d}t = \frac{R_0 t_a}{A\sigma}\Delta\tau = \frac{R_0}{\dot{\tau}}\Delta\tau \quad (9)$$

This result can be interpreted saying that the number of earthquakes triggered by a given stress change in a given area is equal to the number of earthquakes that the same area would have generated during the time necessary to the tectonic load to produce a stress change equal to $\Delta\tau$ at the rate $\dot{\tau}$. This is a simple but relevant result that has important consequences on the building up of the model.

The background seismicity rate, R_0, and the stress rate, $\dot{\tau}$, are not independent in a specific area. Under a number of assumptions, it can be shown (see Appendix A) that these two parameters are related by the following relationship:

$$\dot{\tau} = R_0\pi\frac{b}{1.5-b}\left(\frac{7}{16}M_0^*\right)^{2/3}\Delta\sigma^{1/3}10^{(1-b)(m_{max}-m_0)} \quad (10)$$

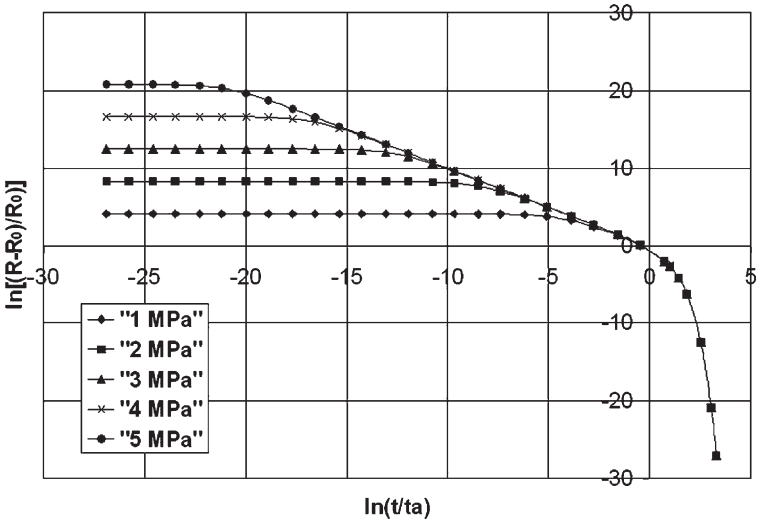

Fig. 1. Theoretical time-distribution of the triggered seismicity rate, R', for different values of induced shear stress, $\Delta\tau$. The values of the parameters used are: $R_0=2$ events/year, $A\sigma=0.24$ MPa, $\dot{\tau}=5$ kPa/year.

where b is the slope of the G–R law, M_0^* is the seismic moment of an earthquake of magnitude m_0[1], $\Delta\tau$ is the stress drop (supposed constant for all the earthquakes), and m_0 and m_{max} are the minimum and maximum magnitudes, respectively. The difference $m_{max}-m_0$ is not critical for the results because it is multiplied by $(1-b)$, a factor close to zero if, as normally is the case, b is close to 1.

We want to introduce the rate-and-state constitutive law in stochastic models such as that expressed by Eqs. (3) (4) (5) and (6a) and (6b), so as to allow the computation of the likelihood of a seismic catalog under the new model. The stress change $\Delta\tau$ caused at any point by any earthquake should be computed taking into account the focal parameters and the source mechanism of each earthquake. This information is not usually contained in an earthquake catalog. Here we introduce a shortcut that allows the use of the most common catalog information constituted just by the origin time, epicentral coordinates and magnitude. Empirically we hypothesize that the stress change produced by an earthquake is given by

$$\Delta\tau = \Delta\tau_0 \left(\frac{d_i^2}{r^2 + d_i^2} \right)^q, \tag{11}$$

where r, d_i and q have the same meaning as in Eq. (6b) and $\Delta\tau_0$ is a free parameter representing the maximum shear stress produced by the fault at its epicenter. Eq. (11) implies a strong simplification of the Coulomb stress pattern, by ignoring the typical azimuthal dependence with negative "lobes". This rather crude assumption can be used as a first approximation, taking into account the experimental difficulties found in observing stress shadows and the importance of location errors for the computation of the stress change induced by small ($m<5$) quakes (Marsan, 2003; Helmstetter et al., 2005). The circular symmetry expressed by Eqs. (6a) and (6b) is so retained in Eq. (11). Note that if $q=1.5$, Eq. (11) is consistent with the physical requirement of the r^{-3} decay of the stress for $r\to\infty$ expected for a double–couple source in an elastic medium (see also Dieterich, 1995). We guess that d is related to the magnitude m of the earthquake and make the hypothesis that

$$d^2 = d_0^2 10^{(m-m_0)}, \tag{12}$$

where d_0 is the radius of a circular fault of magnitude m_0. Eq. (12) can be simply derived from the expression of the seismic moment for a circular fault in terms of stress drop and source radius (Keilis-Borok, 1959):

$$M_0 = \frac{16}{7}\Delta\sigma d^3 \tag{13}$$

and the relation between the seismic moment M_0 and the magnitude m of an earthquake:

$$M_0 = M_0^* 10^{1.5(m-m_0)} \tag{14}$$

with the previous meaning of M_0^* and m_0.

Taking into account the result of Eq. (9) by integration of Eq. (11) over the whole (x, y) plane, we obtain that the total number of aftershocks triggered by an earthquake is:

$$N_{tot} = \frac{r_0}{\dot\tau}\int_{-\infty}^{+\infty}\int_{-\infty}^{+\infty}\Delta\tau\,dx\,dy = \frac{r_0\Delta\tau_0}{\dot\tau}\frac{\pi}{q-1}d^2. \tag{15}$$

The total number of aftershocks is so proportional to the source area and, as a consequence of Eqs. (13) and (14), to 10^m or to $10^{2/3M_0}$. Note that in order to obtain this result we have assumed the hypothesis of a bi-dimensional distribution of sources, as discussed by Helmstetter et al. (2005). However, this result is consistent with empirical observations (Vere-Jones, 1969; Helmstetter and Sornette, 2002; Felzer et al., 2002) and the theoretical results obtained by Console and Catalli (submitted for publication) for simulations with rectangular faults.

Now we can reformulate the epidemic model of Eq. (3) by replacing $\lambda_i(x,y,t,m)$ with the net triggered occurrence density rate obtained multiplying $R'(t-t_i) = R(t-t_i)-R_0$ by β for each earthquake of the catalog occurring at the time t_i. R_0 assumes the meaning of the background occurrence rate $\mu(x,y,m)$. For numerical applications it is necessary to define the value of the various parameters appearing in Eqs. (7), (8), (10), (11) and (12). Note that A and σ appear multiplied everywhere, so that they don't constitute independent parameters. In this study we aim at reducing the number of free parameters as far as possible, so we arbitrarily fix the value of some parameters that can be guessed by the experience:

$\Delta\tau$, the source stress drop, is fixed equal to 2.5 MPa (Dieterich, 1994);
q is fixed equal to 1.5, for consistency with the theory of elasticity when $r\to\infty$;
b, m_0 and m_{max} depend on the catalog used;

[1] In this paper we assume the validity of the relation $M_0=10^{9.1+1.5m}$(Nm) (Hanks and Kanamori, 1979).

R_0 is obtained from the studied catalog by means of a smoothing algorithm (Console and Murru, 2001).

We leave only $\Delta\tau_0$ and the product $A\sigma$ as free parameters of the new model, to be determined by a maximum-likelihood best fit.

4. Testing the models with the seismicity of Japan

The procedure adopted in this study reflects that used by Console and Murru (2001) and Console et al. (2003) and previously introduced by Ogata (1998). It consists in searching for the maximum of the log-likelihood function of a realization of seismic events described by a catalog $\{x_j, y_j, t_j, m_j, j=1,\ldots, N\}$:

$$\ln L = \sum_{j=1}^{N} \ln[\lambda(x_j, y_j, t_j, m_j)V_0] - \int_X \int_Y \int_T \int_M \lambda(x, y, t, m)\mathrm{d}x\mathrm{d}y\mathrm{d}t\mathrm{d}m, \quad (16)$$

where $V_0=\int_X \int_Y \int_T \int_M \mathrm{d}x\mathrm{d}y\mathrm{d}t\mathrm{d}m$ is a coefficient whose dimensions are equal to those of the inverse of the rate density $\lambda(x_j,y_j,t_j,m_j)$.

The second term at the right-hand side of Eq. (16), expressing the expected total number of triggered events, should be computed on the total space-time-magnitude volume spanned by the catalog. For saving computation time, we make an estimate in excess of the integral over the space, by assuming it equal to the integral over the whole (x, y) plane.

Here we are aiming to establishing the predictive power of the models for earthquakes of significant impact on the population. In this sense we don't want to limit the use of the epidemic model to forecasting conventional aftershock activity soon after main shocks, but we want to emphasize also its capacity of forecasting main shocks that occur after foreshocks. To do so, we decided to consider the likelihood of the observed earthquakes under the respective models taking as target events only the strongest earthquakes, and we arbitrarily selected for them the magnitude threshold $m_m=6.5$. In this way, the sum in the first member of the right side of Eq. (16) and the integral in the second member are computed only for the earthquakes with magnitude $m \geq 6.5$, but the occurrence rate density is computed taking into account the triggering effect of all the earthquakes exceeding magnitude m_0.

The method outlined above has been implemented on the seismic catalog collected by the Japan Meteorological Agency (JMA) from January 1, 1970 to December 31, 2003, containing 33,346 earthquakes of magnitude equal to or larger than 4.0. On the basis of an analysis of completeness, we have selected the events with magnitude $m \geq 4.5$ and depth $h \leq 70$ km contained in the polygon 30–46°N latitude and 128–150°E longitude. This selection reduces the data set to a number of

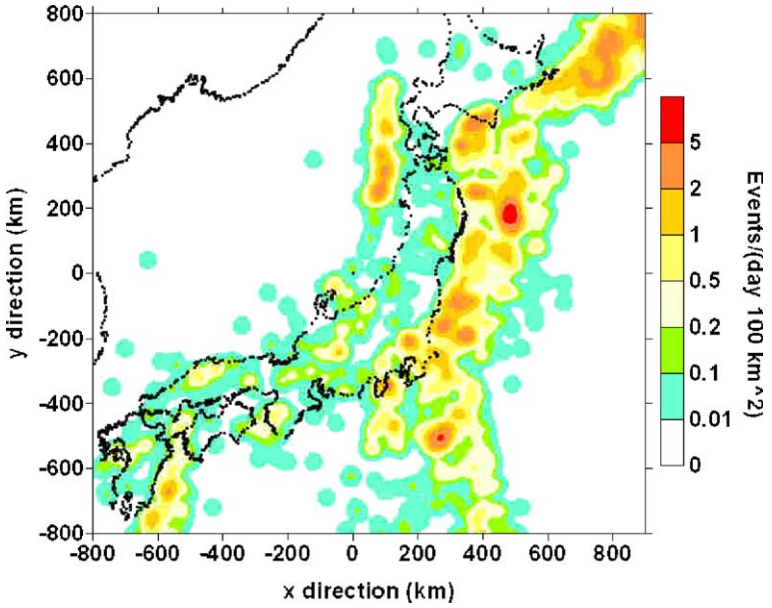

Fig. 2. Smoothed seismicity of the Japan area for the period 1 January 1970–31 December 2003, using 20 km as the value of the correlation distance. The color scale represents the average number of earthquakes ($M \geq 4.5$ and $h \leq 70$ km) in an area of 100 km^2, over the whole time period spanned by the catalog. The origin of the rectangular coordinates is in the point 38°N, 144°E.

7467 events. The largest recorded magnitude is $m_{max}=8.2$. The maximum-likelihood b-value of the data set is 0.881 ± 0.011, with the error computed using the formula suggested by Shi and Bolt (1982).

The wideness of the geographical region used in this exercise reflects the generality of the epidemic algorithm, which is capable of fitting the seismicity in various situations, without the necessity of being tuned on the features of specific environments.

The catalog has been divided in two parts: a learning period from 1970 to 1993 and a test period from 1994 to 2003. This choice has been guided by the criterion that each of the periods included enough events to achieve a good reliability of the results. The first part of the catalog (learning data set), containing 4671 events of magnitude $m\geq4.5$ and 43 events of magnitude $m\geq6.5$, has been used for the best fit of the free parameters characterizing models ETASa, ETASb and ERS, respectively. The maximum-likelihood b-value of the learning data set is 0.924 ± 0.011. The second part (testing data set), containing 2796 events of magnitude $m\geq4.5$ and 28 events of magnitude $m\geq6.5$, has been used for the evaluation of the likelihood for the three models in a forward-retrospective way. In this way the requirement that the test is carried out on a data set independent of that on which the hypothesis is formulated, is fulfilled.

The space density of earthquakes of magnitude equal to or larger than m_0, $\mu_0(x,y)$, for the learning data set has been computed by interpolation of a grid of 10 by 10 km. The values at each node of the grid have been obtained by a smoothing algorithm over all the events of this data set with a correlation distance of 20 km (Console and Murru, 2001). Fig. 2 shows the plot of $\mu_0(x,y)$ for the learning set.

The maximum-likelihood best fit for model ETASa has provided the following results:

$K=0.00760$ days^{p-1}, $d=5.91$ km, $q=1.757$, $c=0.0158$ days, $p=1.244$. They yield a failure rate $f_r=0.580$ and a maximum log-likelihood $\ln L_a=305.44$.

For model ETASb we have found the following maximum-likelihood parameters:

$K=0.000566$ days^{p-1}, $d_0=2.522$ km, $q=1.989$, $c=0.0143$ days, $p=1.224$, $\alpha=0.873$. The failure rate is $f_r=0.574$ and the maximum log-likelihood is $\ln L_b=308.88$.

For model ERS, having chosen $m_0=4.5$ (from which $M_0^*=7.06\ 10^{15}$ Nm and $d_0=1.07$ km have been

Table 1
List of the 28 target events, and their occurrence rate density (events/day/km^2) under the Poisson model, model ETASb and model ERS, respectively

Date	Coordinates	M	λ_0	λ_b	λ_{ERS}	λ_{ERS}/λ_b
08/04/1994	40.568, 143.957	6.5	6.1E−08	3.5E−08	3.3E−08	0.932
04/10/1994	43.372, 147.678	8.2	2.6E−09	1.6E−09	1.5E−09	0.943
05/10/1994*	43.270, 148.468	6.8	1.5E−08	2.1E−05	5.5E−05	2.676
05/10/1994*	43.322, 148.370	6.6	2.3E−08	8.7E−04	3.4E−04	0.391
09/10/1994*	43.555, 147.807	7.3	1.7E−08	2.6E−06	2.3E−06	0.866
28/12/1994	40.427, 143.748	7.6	6.0E−09	3.7E−09	5.8E−09	1.583
29/12/1994*	40.113, 143.023	6.5	4.9E−08	3.0E−06	8.9E−06	2.911
29/12/1994*	40.315, 143.815	6.5	7.2E−08	1.6E−04	3.3E−05	0.205
07/01/1995	40.220, 142.308	7.2	2.4E−08	2.1E−08	7.8E−08	3.662
17/01/1995	34.595, 135.037	7.3	5.4E−11	3.4E−11	3.0E−11	0.882
29/04/1995	43.707, 147.887	6.7	6.8E−08	1.0E−07	3.8E−07	3.635
25/11/1995	44.565, 149.363	6.8	4.9E−08	2.9E−08	2.8E−08	0.969
30/12/1995	40.697, 143.755	6.5	3.3E−08	2.8E−08	7.5E−08	2.716
17/02/1996	37.305, 142.550	6.8	7.3E−09	4.3E−09	5.0E−09	1.158
19/10/1996*	31.795, 132.010	6.9	3.8E−08	8.8E−05	1.1E−04	1.241
03/12/1996	31.765, 131.682	6.7	1.5E−08	1.6E−08	1.3E−07	8.025
26/03/1997	31.968, 130.360	6.6	8.9E−10	6.0E−10	1.2E−09	2.067
25/06/1997	34.438, 131.668	6.6	8.7E−10	5.1E−10	5.2E−10	1.018
28/01/2000	43.005, 146.748	7.0	2.9E−08	1.8E−08	1.6E−08	0.899
01/07/2000*	34.187, 139.197	6.5	1.7E−08	1.5E−05	5.8E−06	0.402
30/07/2000*	33.967, 139.413	6.5	2.9E−08	1.6E−05	1.7E−05	1.067
06/10/2000	35.270, 133.352	7.3	5.5E−09	3.5E−09	3.3E−09	0.924
24/03/2001	34.128, 132.695	6.7	2.1E−09	1.2E−09	2.2E−09	1.764
25/05/2001	44.313, 148.817	6.9	2.5E−08	1.5E−08	1.4E−08	0.979
26/09/2003	41.775, 144.082	8.0	1.1E−09	6.2E−10	6.1E−10	0.994
26/09/2003*	41.707, 143.695	7.1	5.7E−09	1.6E−04	4.7E−05	0.287
29/09/2003	42.357, 144.557	6.5	1.4E−08	5.7E−07	2.7E−06	4.668
31/10/2003	37.828, 142.698	6.8	9.8E−09	6.8E−09	1.7E−08	2.548

computed), and $\alpha=\beta$, these parameters have been obtained:

$\Delta\tau_0=0.75$ MPa and $A\sigma=0.012$ MPa, with a failure rate $f_r=0.437$ and a maximum log-likelihood $\ln L_{ERS}=299.91$.

Note that the log-likelihood for model ERS is slightly lower than those for models ETASa and ETASb. The difference is of the order of few units, not enough to reject any of the three hypotheses in favor of the other according to the Akaike Information Criterion. Note also that the log-likelihood under a time-independent Poisson model on the same catalog is only $\ln Lp=228.02$, so as to allow rejecting this hypothesis in favor of the others.

The test is carried out on a different and independent data set (1994–2003). In the test we run the algorithm for the likelihood computation without looking for a best fit, just using the parameters

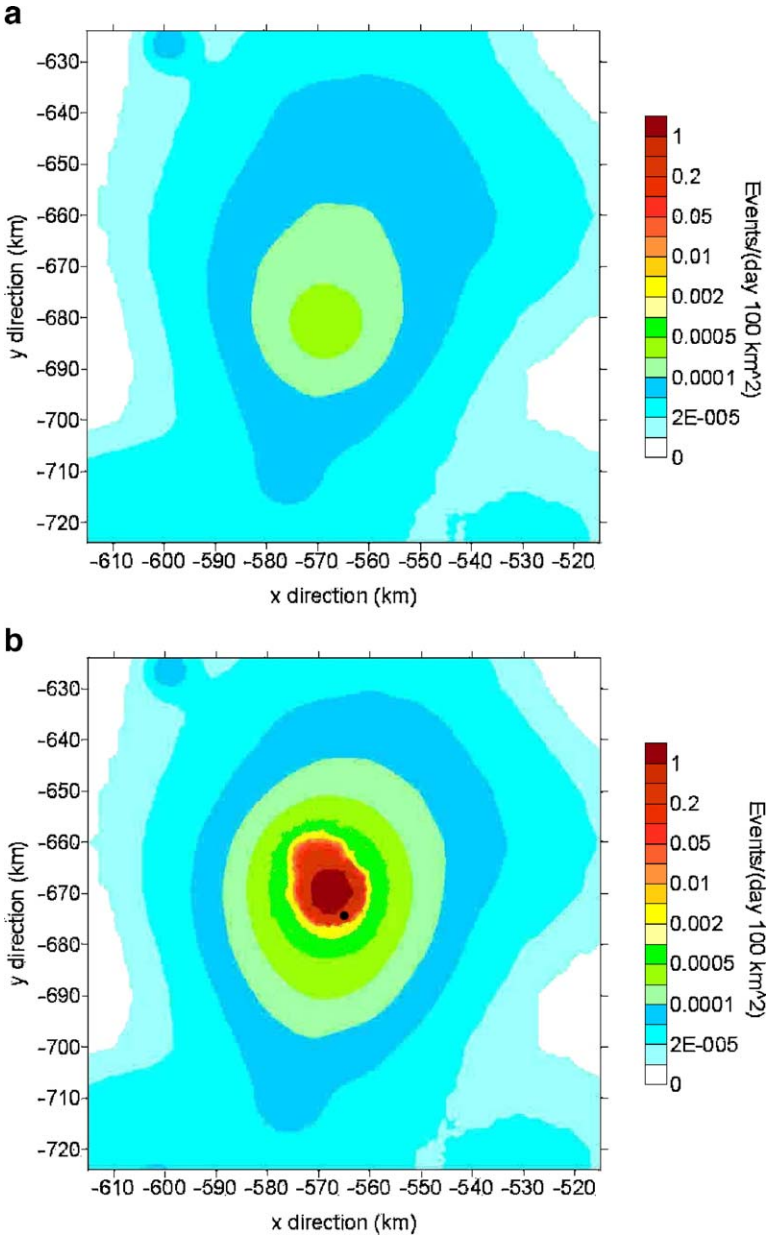

Fig. 3. (a) Modeled occurrence rate density, $M\geq 4.5$, (events/day/100 km^2) on October 19, 1996 at 00:00 UTC. (b) As in (a) but after the occurrence of a few precursory events and just before the earthquake of October 19, 1996 (M 6.9, 23:44 UTC). The epicenter of this earthquake is shown by a black dot. The origin of the rectangular coordinates is the same as in Fig. 2.

obtained from the learning phase. The effective number of free parameters in the test is zero for all the models, so that the Akaike Information Criterion is not applicable. The results are:

Poisson model: $\ln L_p = 111.54$
model ETASa: $\ln L_a = 165.30$
model ETASb: $\ln L_b = 169.81$
model ERS: $\ln L_{ERS} = 171.24$.

Model (ERS) yields a likelihood slightly larger than those of the ETASa and ETASb ones.

A more detailed analysis of the single contribution of each target event to the final value of the log-likelihood can be made by considering the rate density $\lambda_0(x_j, y_j, m_j)$ of the Poisson model and the rate density $\lambda(x_j, y_j, t_j, m_j)$ of the clustering models for each target event. These rates are reported in Table 1 for the whole test period (1994–2003). Table 1 shows that for 9 out of 28 events the rate density computed by both clustering models is by some orders of magnitude larger than that computed by the Poisson model. These events (marked by a star in the first column of Table 1) can be considered as forecasted by the clustering algorithms. However, 6 of these 9 forecasted events occurred in the influence space–time volume of previous larger earthquakes. This was the case of both clusters occurred in 1994 and of the cluster occurred in 2003. In the first case, the October 4, 1994 main shock, M 8.2, off the east coast of Hokkaido, was followed in few days in the same zone by three other earthquakes, M 6.8, 6.6 and 7.3, respectively. In the same year, the December 28, 1994 main shock, M 7.6, off the east coast of Tohoku, was followed in one day by two events, both M 6.5. Finally, the September 26, 2003 event, M 7.1 east of Hokkaido, had been preceded by the M 8.0 main shock, occurred about one hour before. In the case of other two earthquakes, respectively the October 19, 1996 main shock, M 6.9 east of Kyushu, and the July 1, 2000 main shock, M 6.5 south of Tokyo, no larger magnitude earthquakes had been recorded in a short space–time interval before them. Another earthquake of the same magnitude and a high rate density has followed the latter main shock at an epicentral distance of 30 km, after one month. There are, then, 16 earthquakes for which the Poisson rate is larger or similar to the clustering model rate density: these cases can be called failures of predicting. The January 17, 1995, M 7.3 Kobe earthquake is among them.

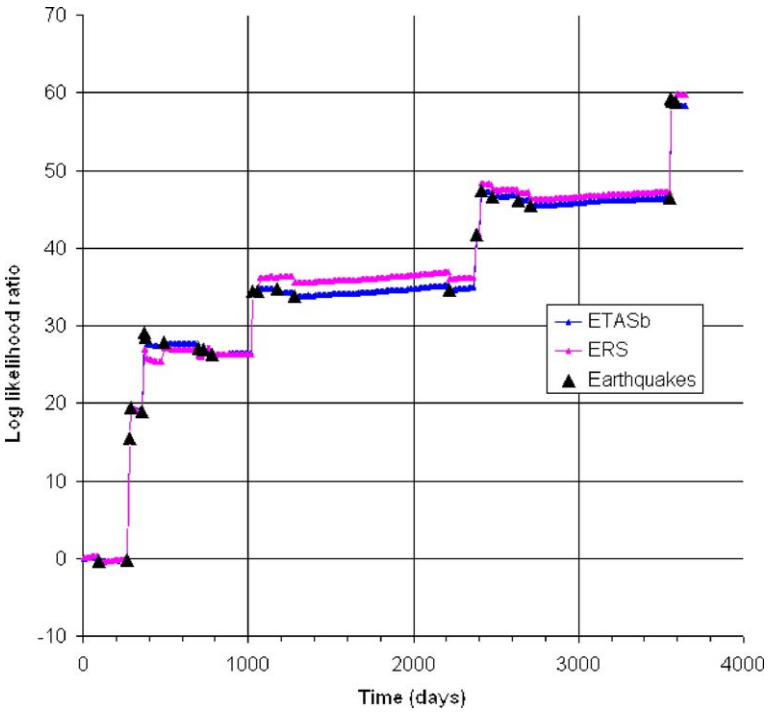

Fig. 4. Log-performance factor achieved by model ETASb and model ERS, respectively, against a plain time-independent Poisson Model, plotted versus time for the whole test period. The origin time is January 1st, 1994 at 00:00 UTC. The occurrence time of the earthquakes with magnitude $M \geq 6.5$ are indicated by black triangles. The sharp positive steps correspond to the events that occurred in a space–time point of large expected rate density with respect to the Poisson model.

The last column of Table 1 reports the ratio between the rate densities of model ERS and model ETASb, respectively. The ratio is larger than 1 if the occurrence rate predicted by model ERS is larger than that predicted by model ETASb. Though the number of cases for which this ratio is smaller or larger than 1 is about the same, the overall better performance of model ERS is due to a few earthquakes for which it achieves a rate several times larger than model ETASb This circumstance applies to earthquakes that occurred later in time and longer on distance from the triggering event, as it can be seen in Table 1 for the earthquakes whose value of λ_{ERS}/λ_b is higher than 2.0.

In Fig. 3a and b we show an example of how the ERS model could be applied in a real case to display the changes of the expected occurrence rate density ($M \geq 4.5$) during the day before the October 19, 1996 event (31.83°N–132.01°E, M 6.9, 23:44 UTC) within a square of 100×100 km. Note that the occurrence rate density before this sequence is not zero but ranges from $1 \cdot 10^{-4}$ to $5 \cdot 10^{-4}$. The values of failure rate f_r, $\Delta\tau_0$ and $A\sigma$ considered for the computation are those obtained by the maximum log-likelihood best fit.

Fig. 4 shows the plot of the log-performance factor for both models ETASb and ERS respect to the time independent Poisson model, versus time for the ten-year test period. Each of the events with magnitude equal to or larger than 6.5 produces a sharp step in the performance factor. The step is positive when the occurrence rate expected by the epidemic model is larger than that expected by the Poisson model. Note the difference in the size of these steps between the two epidemic models. Besides the information contained in Table 1, Fig. 3 puts in evidence also the trend of the performance factor in the time periods between the target events. This trend is negative if the occurrence rate expected by the Poisson model for the whole target area is smaller than that expected by the epidemic model, as it is generally the case.

5. Discussion and conclusions

We have shown how a previously existing clustering model can be modified by the application of the rate-and-state theory. This application has allowed reducing the number of free parameters of the model, giving at the same time a physical meaning to each of them. The application of a unique algorithm to secondary seismic activity triggered by previous aftershocks, implies the existence of an infinite population of faults, some of which are always close to the critical state, even if they belong to segments of fault that have already released their stress.

The time dependence of the triggering effect of the former stochastic epidemic models, described empirically by the Omori law in a unique way regardless of the distance from the triggering event, has been substituted by Eq. (7) derived by Dieterich (1994) for a population of faults. With respect to the Omori law, the rate-and-state model predicts longer durations of constant seismic activity for areas of low Coulomb stress-change.

The application of both the stochastic and the rate-and-state models to the computation of the likelihood of earthquake catalogs implies considerable simplifications of the seismic processes. In order to limit the number of free parameters in both models here we have hypothesized the constancy of the b-value in time and space. So, the b-value has been computed for the catalog as a whole, while the geographical distribution of the time-independent background has been computed on a grid of 10 by 10 km.

Another strong simplification assumed in both models is the circular symmetry of the triggering effects, respectively expressed by Eqs. (6) and (11). A similar simplified approximate representation has been used by Dieterich (1995). Note that in model ETASa Eq. (6a) gives directly the density distribution of triggered events, and d is a constant independent of the magnitude of the triggering earthquake. The best fit of d may reflect the location error of the events in the catalog, especially for small magnitudes. The same applies to d_0 for Eq. (6b) in model ETASb. For model ERS Eq. (11) gives the stress change distribution, and the occurrence rate density is computed through Eq. (7). In this case parameter d_0 depends on the magnitude through Eq. (12) and it is no longer a free parameter. There is no doubt that the stress change computation made by a physical model of each earthquake source would improve the results significantly, but this information is not currently available in a typical seismic catalog.

Any of the models ETASa, ETASb and ERS is consistent with the hypothesis that the number of events directly triggered by an earthquake of magnitude m is proportional to 10^m. This is explicitly stated by Eq. (4) for model ETASa and can be derived from Eq. (6b) for model ETASb. Eqs. (12) and (15) justify this feature for model ERS, as a consequence of the proportionality between the total number of triggered events and the stress change $\Delta\tau$. From a physical point of view, it must be noted that the proportionality between m and the logarithm of the number of triggered events reflects the assumption that these events originate on an active surface and not on the whole three-dimensional volume.

The existing clustering models ETASa and ETASb and their modified version ERS have been tested by the seismic catalog reported by JMA for Japan. A first part of the catalog (1970–1993) has been used in the learning phase for the maximum-likelihood best fit of the free parameters. A second part (1994–2003) has been used for an independent test. This test has shown that the likelihood of the data set under the new physical model ERS is even better than that obtained under the purely stochastic models ETASa and ETASb.

As to the number of events triggered by a previous earthquake, called *aftershock productivity*, we have supposed that this number is proportional to exp(α), with $\alpha=\beta$, for models ETASa and ERS. Model ETASb is the only one where α is obtained by a maximum likelihood best fit, and the value so obtained, nearly three times smaller than β, appears unrealistically small. If this circumstance was real, it would mean as a consequence that small events dominate the process of triggering aftershocks. It seems that this feature is typical of the cases when α is obtained by the maximum likelihood best fit of a catalog (Helmstetter et al., 2005). For instance, Console et al. (2003) obtained 1.0 for the Italian seismicity, and Zhuang et al. (2004) obtained a value around 1.35 for the JMA catalog. There are at least two different possible explanations of such results: one of them might be the lack of aftershocks reported in the catalogs soon after a strong earthquake; the other could be thought as a mathematical artifact caused by the strong correlation between K and α in the best fit regression.

Let's now consider the physical implications of the values obtained for the parameters $\Delta\tau_0$ and $A\sigma$ in model ERS. $\Delta\tau_0=0.75$ MPa (7.5 bars) is a value about three times smaller than the value of the constant stress drop $\Delta\sigma$ assumed in the source model. Though the largest stress change very close to the fault edges, for a constant stress drop dislocation, is expected to be higher, we must also consider that the value obtained from the best fit is an average result of extremely complex real situations. These situations may include strong stress change variations over the fault area, from negative values of the order of $\Delta\sigma$, where the stress drop is total, to larger positive values, in correspondence of barriers. An example of stress change variations over a segment of the Calaveras fault of some tens kilometres length has been reported by Console and Catalli (submitted for publication) in the analysis of the Morgan Hill earthquake.

Our result for $A\sigma$ (0.012 MPa) is smaller but comparable with that (0.04 MPa) obtained by Toda and Stein (2003) in their study of aftershocks triggered by a couplet of earthquakes in Southern Kyushu. It appears consistent with the result obtained by Harris and Simpson (1998), who estimated for $A\sigma$ a range of acceptable values of 0.0012 to 0.6 MPa in a study of earthquake interaction in the San Francisco Bay area.

The value $A\sigma=0.012$ MPa would imply a normal stress σ of the order of only 1 MPa applied to the fault plane, assuming a value of A of the order of 0.01, as obtained by Dieterich (1994) from laboratory experiments. However, Dieterich (1995) assumed values ranging from $A=0.00001$ to $A=0.007$ in his simulations. This wide range of values is consistent with the estimate of a lithostatic normal stress of the order of 300 MPa acting at a depth of 10 km. We may also guess that confined fluids in the fault zone have the effect of significantly lowering the effective normal pressure on the faults.

We conclude noting that the introduction of relatively simple physical constraints allowed a substantial reduction in the number of free parameters necessary in the formulation of stochastic models of seismogenic processes.

Acknowledgements

We are particularly grateful to two anonymous reviewers for their useful advice, constructive comments, and suggestions that have improved the final version of the manuscript.

Appendix A

We want to derive Eq. (10) of the main body of the text, expressing a relation between the background seismicity rate R_0 and the stress rate $\dot{\tau}$ in a given seismic area. We suppose that the seismic area is small enough to justify the assumption of a uniform behavior, but at the same time large enough to allow the assumption of an infinite population of faults with a continuous distribution of parameters.

For a circular fault of radius d the following relations hold among the average dislocation $\Delta\bar{u}$, the stress drop $\Delta\sigma$, the static seismic moment M_0, and the source area S (Keilis-Borok, 1959; Udìas, 1999):

$$\Delta\bar{u} = \frac{16}{7\pi}\frac{\Delta\sigma}{\mu}d, \tag{A1}$$

$$M_0 = \mu\Delta\bar{u}S = \frac{16}{7}\Delta\sigma d^3, \tag{A2}$$

with μ=shear modulus of the elastic medium. We assume the following relation between the magnitude m

and the seismic moment M_0 (Hanks and Kanamori, 1979):

$$M_0 = 10^{9.1+1.5m}. \quad \text{(A3)}$$

The total seismic moment released by a large set of events is:

$$M_{0\text{tot}} = \int_0^{M_{0\max}} M_0 \mathrm{d}N = \int_{-\infty}^{m_{\max}} M_0^* 10^{1.5(m-m_0)} \mathrm{d}N, \quad \text{(A4)}$$

where $M_{0\max}$ is the largest seismic moment, $m_{\max}$ is the largest magnitude of the area, and M_0^* is the seismic moment of an earthquake of magnitude m_0.

We assume the validity of the G–R law for the number of earthquakes of magnitude larger than m:

$$N(m) = N_0 10^{-b(m-m_0)}, \quad \text{(A5)}$$

where N_0 is the number of earthquakes of magnitude larger than m_0. This gives:

$$\mathrm{d}N = b\ln 10 N_0 10^{-b(m-m_0)} \mathrm{d}m. \quad \text{(A6)}$$

Then we obtain:

$$M_{0\text{tot}} = \int_{-\infty}^{m_{\max}} M_0^* 10^{1.5(m-m_0)} b\ln 10 N_0 10^{-b(m-m_0)} \mathrm{d}M, \quad \text{(A7)}$$

and

$$N_0 = \frac{M_{0\text{tot}}}{M_0^*} \frac{1.5-b}{b} 10^{(b-1.5)(m_{\max}-m_0)}. \quad \text{(A8)}$$

In terms of seismic rate R_0 we may also write

$$R_0 = \frac{N_0}{\Delta T S_{\text{tot}}}, \quad \text{(A9)}$$

where ΔT and S_{tot} are, respectively, the total time and the total area where R_0 is averaged.

We may also express the total seismic moment released by a circular seismic area S_{tot} of radius d_{tot} during the time ΔT in terms of the average stress drop $\Delta\bar{\sigma}$, and the stress rate $\dot{\tau}$.

$$M_{0\text{tot}} = \frac{16}{7} \Delta\bar{\sigma}\, d_{\text{tot}}^3 = \Delta T S_{\text{tot}} \frac{16}{7\pi} \dot{\tau} d_{\text{tot}}. \quad \text{(A10)}$$

By elimination of N_0 and $M_{0\text{tot}}$ from (A8), (A9) and (A10) we obtain:

$$\frac{R_0}{\dot{\tau}} = \frac{16}{7\pi} \frac{d_{\text{tot}}}{M_0^*} \cdot \frac{1.5-b}{b} 10^{(1.5-b)(m_{\max}-m_0)}. \quad \text{(A11)}$$

We suppose now that d_{tot} is the equivalent source radius of the earthquake with the largest size of the area, and express it by:

$$d_{\text{tot}}^3 = \frac{7}{16} \frac{M_{0\max}}{\Delta\sigma} = \frac{7}{16} \frac{M_0^*}{\Delta\sigma} 10^{1.5(m_{\max}-m_0)}. \quad \text{(A12)}$$

Finally, by substitution of Eq. (A12) in (A11):

$$\dot{\tau} = \pi R_0 \frac{b}{1.5-b} \left(\frac{7}{16} M_0^*\right)^{2/3} \mathrm{D}\sigma^{1/3} 10^{(1-b)(m_{\max}-m_0)}. \quad \text{(A13)}$$

References

Belardinelli, M.E., Bizzarri, A., Cocco, M., 2003. Earthquake triggering by static and dynamic stress change. J. Geophys. Res. 108, 2135. doi:10.1029/2002JB001779.

Boatwright, J., Cocco, M., 1996. Frictional constraints on crustal faulting. J. Geophys. Res. 101, 13895–13909.

Console, R., Murru, M., 2001. A simple and testable model for earthquake clustering. J. Geophys. Res. 106, 8699–8711.

Console, R., Murru, M., Lombardi, A.M., 2003. Refining earthquake clustering models. J. Geophys. Res. 108, 2468. doi:10.1029/2002JB002130.

Console, R., Catalli, F., submitted for publication. A physical model for aftershocks triggered by dislocation on a rectangular fault. Ann. Geophys.

Dieterich, J.H., 1986. A model for the nucleation of earthquake slip, Earthquake Source Mechanics. Geophys. Monogr. Ser. 37, 36–49.

Dieterich, J.H., 1992. Earthquake nucleation on faults with rate and state dependent strength. Tectonophysics 211, 115–134.

Dieterich, J.H., 1994. A constitutive law for rate of earthquake production and its application to earthquake clustering. J. Geophys. Res. 99, 2601–2618.

Dieterich, J.H., 1995. Earthquake simulations with time-dependent nucleation and long-range interactions. Nonlinear Process. Geophys. 2, 109–120.

Dieterich, J.H., Cayol, V., Okubo, P., 2000. The use of earthquake rate changes as a stress meter at Kilauea volcano. Nature 408, 457–460. doi:10.1038/35044054.

Felzer, K.R., Becker, T.W., Abercrombie, R.E., Ekstrom, G., Rice, J.R., 2002. Triggering of the 1999 M_w 7.1 Hector Mine earthquake by aftershocks of the 1992 M_w 7.3 Landers earthquake. J. Geophys. Res. 107 (B9), 2190. doi:10.1029/2001JB000911.2002.

Gomberg, J., 2001. The failure of earthquake failure models. J. Geophys. Res. 106 (B8), 16253–16263.

Gomberg, J., Beeler, N., Blanpied, M., Bodin, P., 1998. Earthquake triggering by transient and static deformations. J. Geophys. Res. 103, 24411–24426.

Gomberg, J., Beeler, N., Blanpied, M., 2000. On rate and state and Coulomb failure models. J. Geophys. Res. 105, 7857–7871.

Harris, R.A., 1998. Introduction to special section: stress triggers, stress shadows, and implications for seismic hazard. J. Geophys. Res. 103, 24347–24358.

Harris, R.A., Simpson, R.W., 1998. Suppression of large earthquakes by stress shadows: a comparison of Coulomb and rate-and-state failure. J. Geophys. Res. 103, 24439–24451.

Hanks, T.C., Kanamori, H., 1979. A moment magnitude scale. J. Geophys. Res. 84, 2348–2350.

Helmstetter, A., Sornette, D., 2002. Subcritical and supercritical regimes in epidemic models of earthquake aftershocks. J. Geophys. Res. 107 (B10), 2237. doi:10.1029/2001JB001580.

Helmstetter, A., Kagan, Y.Y., Jackson, D.D., 2005. Importance of small earthquakes for stress transfers and earthquake triggering. J. Geophys. Res. 110, B05S08. doi:10.1029/2004JB003286.

Keilis-Borok, I., 1959. On estimation of the displacement in an earthquake source and of source dimensions. Ann. Geofis. 12, 2205–2214.

Kilb, D., Gomberg, J., Bodin, P., 2002. Aftershock triggering by complete Coulomb stress changes. J. Geophys. Res. 107. doi:10.1029/2001JB000202.

King, G.C.P., Cocco, M., 2001. Fault interaction by elastic stress changes: new clues from earthquake sequences. Adv. Geophys. 44, 1–39.

Marsan, D., 2003. Triggering of seismicity at short time scales following California earthquakes. J. Geophys. Res. 108, 2266. doi:10.1029/2002JB001946.

Mendoza, C., Hartzell, S.H., 1988. Aftershock patterns and main shock faulting. Bull. Seismol. Soc. Am. 78, 1438–1449.

Ogata, Y., 1983. Estimation of the parameters in the modified Omori formula for aftershock frequencies by the maximum likelihood procedure. J. Phys. Earth 31, 115–124.

Ogata, Y., 1988. Statistical models for earthquake occurrence and residual analysis for point process. J. Am. Stat. Assoc. 83, 9–27.

Ogata, Y., 1998. Space-time point-process models for earthquake occurrences. Ann. Inst. Stat. Math. 50, 379–402.

Ruina, A., 1983. Slip instability and state variable friction laws. J. Geo>phys. Res. 88 (B12), 10359–10370.

Shi, Y., Bolt, A., 1982. The standard error of the magnitude-frequency *b* value. Bull. Seismol. Soc. Am. 72, 1677–1687.

Stein, R.S., Barka, A.A., Dieterich, J.H., 1997. Progressive failure on the North Anatolian Fault since 1939 by earthquake stress triggering. Geophys. J. Int. 128, 594–604.

Stein, R.S., 1999. The role of stress transfer in earthquake occurrence. Nature 402, 605–609.

Toda, S., Stein, R.S., Reasemberg, P.A., Dieterich, H., Yoshida, A., 1998. Stress transferred by the 1995 M_w=6.9 Kobe, Japan, shock: effect on aftershocks and future earthquake probabilities. J. Geophys. Res. 103, 24543–24565.

Toda, S., Stein, R.S., Sagiya, T., 2002. Evidence from the AD 2000 Izu Islands earthquake swarm that stressing rate governs seismicity. Nature 419 (6902), 58–61 (Sep 5).

Toda, S., Stein, R.S., 2003. Toggling of seismicity by the 1997 Kagoshima earthquake couplet: a demonstration of time-dependent stress transfer. J. Geophys. Res. 108, 2567. doi:10.1029/2003JB002365.

Udìas, A., 1999. Principles of Seismology. Cambridge University Press.

Vere-Jones, D., 1969. A note on the statistical interpretation of Bath's Law. Bull. Seismol. Soc. Am. 59, 1535–1541.

Zhuang, J., Ogata, Y., Vere-Jones, D., 2004. Analyzing earthquake clustering features by using stochastic reconstruction. J. Geophys. Res. 109, B05031. doi:10.1029/ 2003JB002879.

Ziv, A., 2003. Foreshocks, aftershocks, and remote triggering in quasi-static models. J. Geophys. Res. 108 (B10), 2498. doi:10.1029/2002JB002318.

Ziv, A., Rubin, M., 2003. Implication of rate-and-state friction for properties of aftershock sequence: quasi-static inherently discrete simulations. J. Geophys. Res. 108 (B1), 2051. doi:10.1029/2001JB001219.